Vehicle controllability assessment using detailed multibody vehicle simulations

Chrysakis, G. , Monkhouse, H. and Kanarachos, S.

Published version deposited in CURVE October 2015

Vehicle Controllability Assessment Using Detailed Multibody Vehicle Simulations

G. Chrysakis* H. Monkhouse **
S. Kanarachos ***

*Mechanical Automotive Manufacturing Department, Coventry University,
Coventry, CV1 5FB, UK (Tel: +44 (0) 2477658377; e-mail: g.chrysakis@coventry.ac.uk)
** Protean Electric Limited, Farnham, Surrey, GU10 5EH,
UK, (e-mail: helen.monkhouse@proteanelectric.com)
*** Mechanical Automotive Manufacturing Department, Coventry University,
Coventry, CV1 5FB, UK (Tel: +44 (0) 2477657720; e-mail: stratis.kanarachos@coventry.ac.uk)}

Abstract: ISO 26262, the functional safety standard for automotive electric and electronic (E/E) systems, requires a controllability assessment to be made as part of the hazard and risk classification process. As well as influencing the function's Automotive Safety Integrity Level (ASIL), the verifiable controllability may also limit the functions intervention options and intensity during normal operation. For electric driven vehicles this limits their accident-avoidance/-mitigation potential. For an in-wheel motor driven electric vehicle it is questioned whether the failure of a motor could lead to a risk. It is obvious that the result of the risk assessment depends on the operating scenarios chosen. As numerous factors define a driving situation, the possible detailing of these factors is unlimited. In a previous paper, the results of a study regarding the controllability of a vehicle driven by in-wheel motors using a simplified linear bicycle model were presented. In this paper we extend the previous work by qualitatively and quantitatively identifying the hazards associated with in-wheel motors and by quantify the vehicle level effects that could be expected using validated detailed multibody vehicle models in both straight line and cornering events.

Keywords: vehicle controllability, vehicle dynamics, ISO26262, in-wheel motors, multibody vehicle simulations.

1. INTRODUCTION

For public traffic it is necessary to prove that the residual risk, due to hazardous failures or unintended reactions of automotive systems, is acceptably low. Requirements for the risk assessment of safety-related electric and electronic systems in case of failure are provided in ISO 26262 (ISO 26262: 2011).

Electric in-wheel drive systems are flexible, modular vehicle propulsion systems that revolutionize the way vehicles are driven today. Among their advantages are increased manoeuvrability and design freedom, and a reduction in the packaging space required. In-wheel drive systems need to comply with ISO 26262 and therefore research needs to be undertaken to ensure sufficient system safety (Hirano 2012), (Watts et al. 2010). Of concern is the case where one motor fails - besides not meeting the vehicle's acceleration/deceleration requirements - a yaw moment is introduced which acts as a disturbance and causes the vehicle unintendedly to turn. A question that arises during early risk analyses of such a system is the controllability of such system hazards. While this question is answered subjectively in early stages, very often using worst-case risk graphs, the question comes back later in a much more precise way: in cases where an in-wheel motor component failure would produce a deviation between desired and actual vehicle position, and that deviation can be measured in terms of amplitude and/or time, how much deviation can be controlled by the driver? (Reinelt et al. 2006)

A literature survey has shown that similar questions have arisen for active steering systems, automatic braking systems, and active safety systems (Neukum et al. 2008), (Weitzel et al. 2013). In many cases empirical studies have been conducted that assessed the controllability using a group of drivers and vehicles. Objective and subjective measurements have led to the definition of maximum allowable limits for different vehicle dynamics metrics e.g. yaw disturbance.

As numerous factors define a driving situation, the possible detailing of these factors is unlimited. A side-effect of increased detailing is to decrease the rate of occurrence of single situations; thereby lowering the perceived risk and overall safety level required. Hence, a method is needed that allows for the systematic and verifiable derivation of test situations, including traceability of the detailing. Automated controllability assessment using numerical models might be a possible solution, in case they represent reality well.

In a previous paper, the results of a study regarding the controllability of a vehicle driven by in-wheel motors using a simplified bicycle model have been presented and discussed

(Ellims et al. 2013). It is well known that the validity of the bicycle model is restricted only in the linear range e.g. for lateral accelerations up to 0.4g and in case of dry road conditions (Kanarachos 2009). In this paper, we extend the previous work by identifying the hazards associated with in-wheel motors and by quantifying the vehicle level effects that could be expected using validated detailed multibody vehicle models. Furthermore, we expand the risk analysis scope by considering that the vehicle is equipped with an electronic stability control system, like in (Alirezaei et al. 2013), which is now mandatory in Europe.

The rest of the paper is organized as follows: In the second chapter the problem is formulated by presenting the vehicle, driver, driveline and motor failure models used. In Section 3 the scenarios used for evaluating the controllability are described and the maximum allowable limits are shown. These scenarios include the application of torque applied due to fault of the in-wheel motor electric driveline during straight line and cornering events at 150 km/h. The response of the vehicle during low mu surface is also investigated. Section 4 the numerical results are illustrated and discussed while in Section 5 conclusions are drawn.

In order to reduce the risk of a system component failure two possible options exist. The first is to make the component physically redundant (Hirano 2012). The second one it to reallocate the control commands to the remaining actuators in such a way that risk is minimized (Watts et al. 2010). In case, of an electric vehicle driven by one or two pairs of in-wheel motors the redundancy exists.

2. CASE STUDY DEFINITION

2.1 Vehicle Specifications

The multibody model selected represents a GAC Trumpchi. The vehicle is selected as an average sedan vehicle with rear wheel drive (RWD) internal combustion driveline, also equipped with in-wheel motors at each rear wheel (RWDEV). The vehicle specifications used are:

- Aggregate mass: 1870kg

- Front / Rear weight distribution: 53.86% / 46.14%

- Wheelbase: 2.7m

For the scenarios evaluated in this paper the internal combustion driveline is considered to be inactive. Only the in-wheel electric motors propel the vehicle. The in-wheel electric motors used are from Protean Electric and their performance is shown in Figs. 1 and 2.
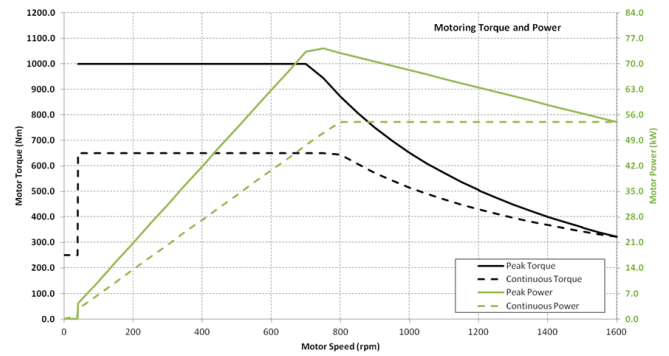

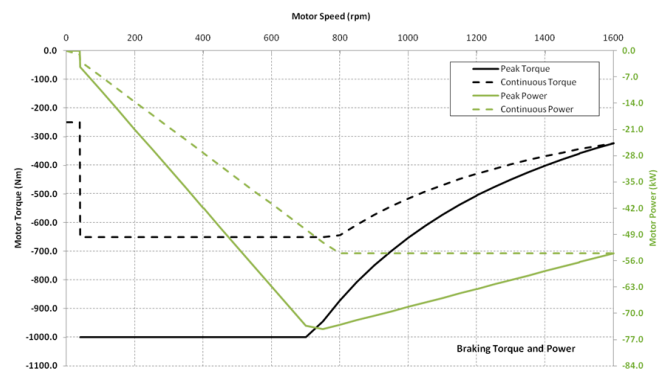Fig. 1. Driving performance of the in-wheel electric motor

Fig. 2. Braking performance of the in-wheel electric motor

2.2 Electric motor failure scenarios

Two electric motor failure scenarios are evaluated. The first scenario is an almost instantaneous increase of the braking force by the motor, followed by controlled decay within 1.5 seconds as shown in Fig. 3. This is performed while the vehicle attempts to maintain velocity during the event. The reason for 'switching off' the torque after a time period is simply that the response of the driver controller to a fixed torque that remains on, is relatively straightforward and the driver is able to control the vehicle with much more ease. The removal of the failure torque is, in reality a much more likely scenario as the vehicle electronics will have intervened. The duration of the time before the fault is injected is simply to allow the vehicle to settle and the use of 10 seconds is arbitrary – it facilitates location of the fault in the results. The vehicle usually starts 'in the air and at speed' and some time is required at the start of the simulation for the tyre forces to initialise and also for the controller gains to take appropriate control of the model. This is to prevent the controller 'battling' the fault and is more reflective of the operator removing drive torque upon detection of a problem.
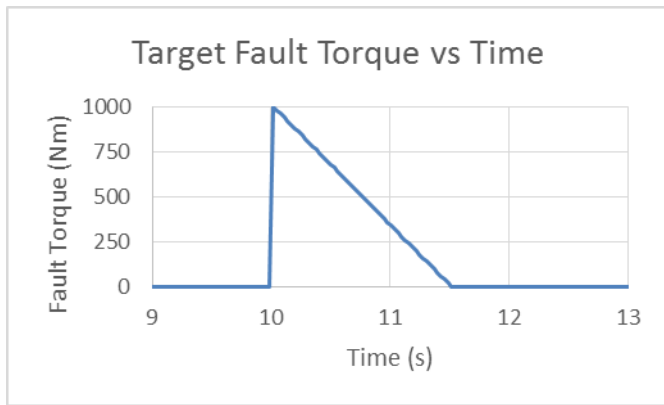
Fig. 3. Intermittent fault torque target versus time

The fault torque applied is limited by the performance of the motor. The target maximum torque is selected according to the maximum torque the motor can provide. However, following the maximum power profile of the motor, the maximum torque applied in this scenario is limited according to the angular velocity of the motor (Fig. 4).
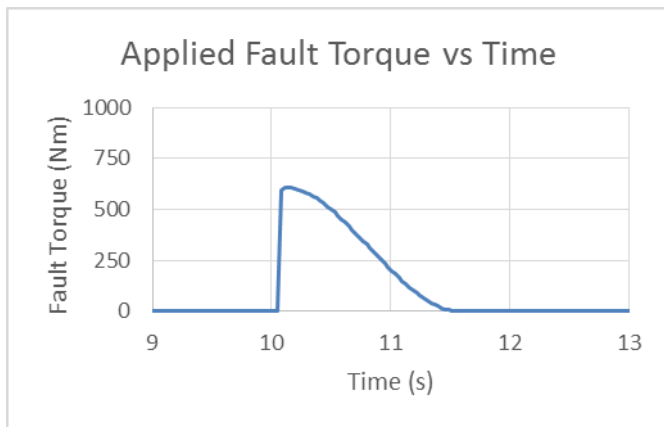

Fig. 4. Applied intermittent fault torque versus time

The second scenario represents a failure of the inverter controlling the electric motor. In case of an inverter failure the control of the electronics is disabled and a passive return of current from the motor to the battery. The magnitude of the current of the system is defined by the difference of the back- electromotive force generated by the motor relative to the voltage of the tractive system energy accumulator. In this scenario the motors are driven at their maximum power rating until the fault occurs. The failure is initially applied to the internal wheel (rear left) motor. The safety monitoring system recognises the torque difference across the axle and disables the second motor across the axis (rear right) after 200ms (Fig. 5) in order to minimise the yaw momentum applied on the vehicle.
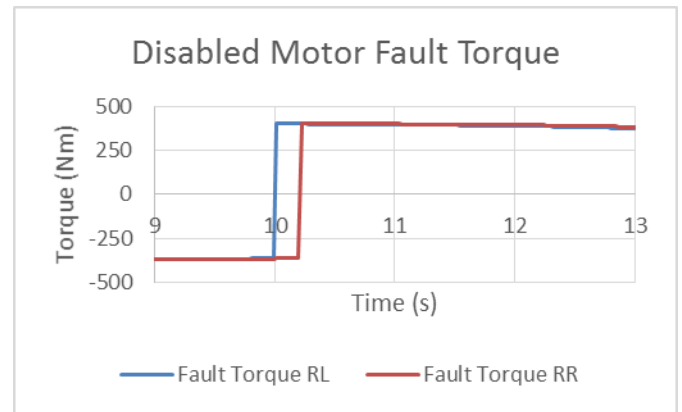

Fig. 5. Torque application due to disabled motors

2.3 Driver model

A detailed analysis with a 2 degree of freedom (Harty & Gade, 2013) vehicle model reveals that in order to reproduce the Neukum results the simplified PID Heading Controller (outlined in Fig. 6 below) has an infinite bandwidth – in other words, the response of the operator is simply too good to reflect a typical driver and some tuning of the model is required. Consequently, the controller model is tuned (via a second order differential equation) to have a specific natural frequency at 2Hz and some damping ratio.
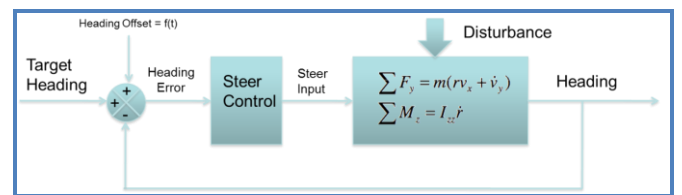

Fig. 6. Heading control model to represent the human operator defined by Neukum.

For the straight line event the model behaves very well. However for the cornering event the filter implementation applied delays the response of the driver. This results in a non-decaying oscillation of the steering input (and of the vehicle) which human drivers would eventually damp out by minimising both the steering torque input and the applied steering angle oscillation amplitude. This is implemented by an additional low gain PID controller controlling the angle of the steering wheel that corresponds to cornering yaw rate. This steering angle controller is tuned in line with the heading controller in order to damp the steering angle oscillation while having minimum impact on the response of the driver due to the fault.

3. SCENARIO DEFINITIONS

The scenarios investigated include the application of fault torque as described in section 2, during straight line and cornering events at initial speed of 150 km/h. The cornering event target is 0.4g of lateral acceleration. The response of the vehicle during low mu surface is also investigated up to the point that the vehicle stability is compromised when an Electronic Stability Control (ESC) system is also applied.

The 10 seconds fault injection is selected in order to allow the vehicle model and controllers to settle.

For the first fault scenario the fault is applied to the rear left motor. The same motor is again used as the disabled motor in the second scenario. The rear left motor is selected due to the increased yaw moment it applies during the failure as in Fig. 7. When a motor fault torque is applied a negative longitudinal force component is applied at the tyre's contact patch proportional to the radius of the tyre. The applied longitudinal force component applies yaw moment, in relation to the distance from the centre of mass, but also as a reduction of the lateral forces at rear axle compared to the front axle because of the friction ellipse. During the second fault scenario, the reduction of the lateral force due to the longitudinal component is similar before and after the fault application due to the similar absolute torque applied. However, the yaw moment caused by the longitudinal force component is still applied because of the opposite torque application across the rear axle. In addition due to the reversal of the longitudinal acceleration vector there is a longitudinal load transfer, unloading the rear tyres and loading the front ones affecting the peak lateral force capability of the tyres.
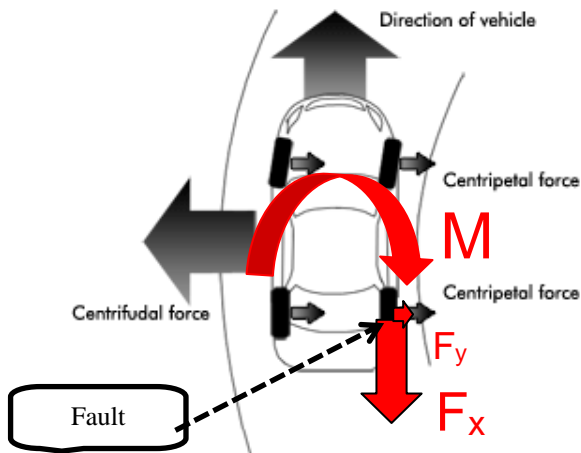

Fig. 7. Yaw disturbance caused by a motor's fault torque

According to Neukum, the peak yaw rate induced for irreversible steering fault at 150 kph is 2.5 deg/s, beyond which the safety of the vehicle is deemed unstable and difficult to control by the driver..

4. RESULTS

4.1 Straight line scenarios

The first set of scenarios are set on a straight line at 150km/h and only high coefficient of friction with the road mu = 1 is considered. Fig. 8 demonstrates the results of the intermittent fault application and Fig. 9 the results during the motor disabling sequence.
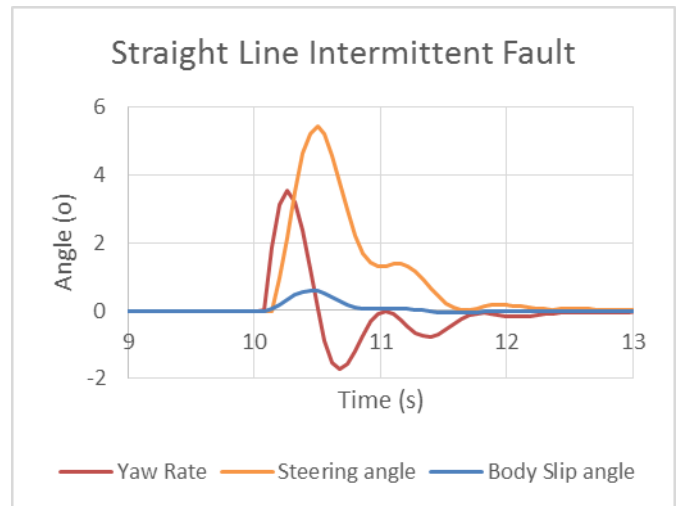

Fig. 8. Straight line performance with intermittent fault

During the intermittent fault at straight line it is understood that the fault injection creates a yaw moment that disturbs the vehicle. The sudden wheel deceleration accelerates the yaw rate up to 3.5º which is above the threshold defined by Neukum, but drops to -1.7º within 0.35s. However the body slip angle raises to only 0.6º posing no controllability issues. The amplitude of the yaw rate and body slip angle reduce to significantly low values as the fault torque also reduces and return back to normal within a second after the end of the fault torque. This scenario does not reflect any controllability issues.
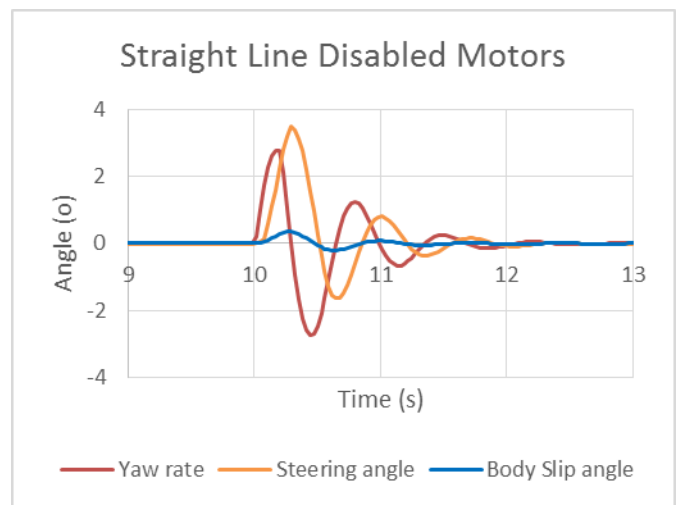

Fig. 9. Straight line performance with disabled motors

Compared to the intermittent fault, disabling permanently the motor creates a yaw moment that raises the yaw rate to 2.7º due to the longitudinal force created by the braking fault torque. However, the safety monitoring system disables the second motor across the driving axle creating a balance of longitudinal forces across the driving axle, canceling the yaw moment due to differential braking. This creates a decaying oscilation of the yaw rate and the body slip angle. The oscilation amplitude of the body slip angle ranges from 0.35º

to -0.2º. The vehicle returns back to its initial stability state at a similar time as the intermittent fault despite the different nature of the fault. This scenario does not reflect any controllability issues.

4.2 Cornering scenarios

4.2.1 Intermittent fault torque

For the cornering scenarios the two types of motor fault are investigated separately. Starting with the intermittent fault the model has been tested in numerous road friction coefficients before selecting the results demonstrated in this paper. At high mu the vehicle does not pose any risk of controllability as it is demonstrated in Fig. 10. The range of added yaw rate is 2.8º to -2.3º and added body slip angle is 0.42º to -0.13º which is slightly above Neukum's range of a permanent fault, however the above mentioned peak values are experienced for a very short time and decay with a high damping ratio.

The tyres operate within to just above their linear region entering without requiring disproportional increase of slip angle in order to provide the additional required lateral force for the stability of the vehicle. At lower mu scenarios the tyre is already operating at its non-linear region and close to its friction limit. At the high mu scenario the yaw moment developed by the reduction of lateral forces due to the fault times the wheelbase is less significant compared to the yaw moment produced by the longitudinal force applied by the fault torque times the halftrack distance. This is because the tyre operates within the linear region of its cornering stiffness and the additional longitudinal force due to the fault will not affect significantly the lateral forces applied. On low mu scenarios however, as the tyre is operating closer to its friction limit, any additional longitudinal forces will significantly reduce the lateral forces as the combined force applied by the tyre will reach the friction limit.

The above is demonstrated in Fig. 11, where the vehicle is controllable until the application of the intermittent fault when the yaw moment applied cannot be controlled because of the lack of the rear tyres to produce any additional lateral forces. The sudden increase of both the yaw rate and body slip angle demonstrate the loss of control of the vehicle despite the efforts of the driver. It should be noted that the response time of the driver is aided by the behaviour of the vehicle as with the increase of yaw rate due to the fault, the steering wheel feedback torque is also increased.
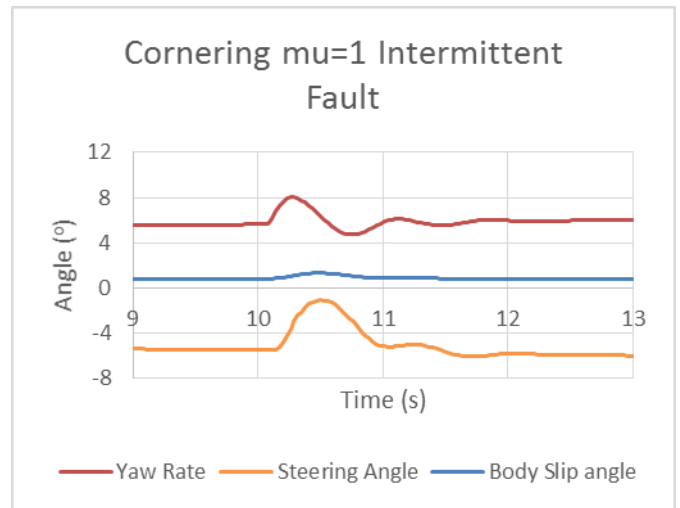

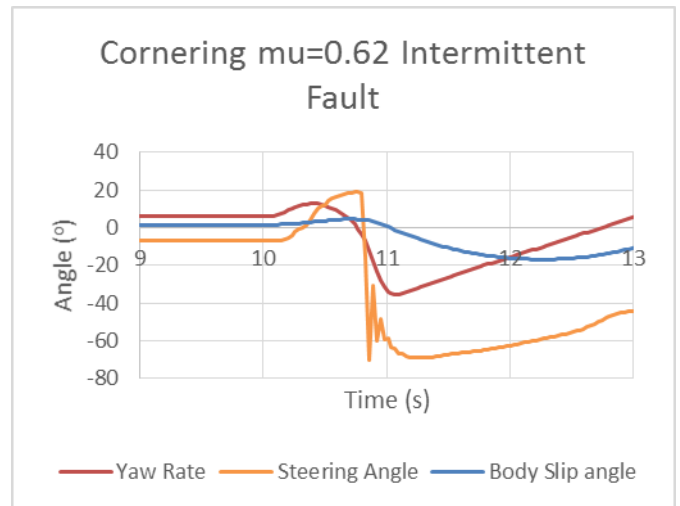Fig. 10. Cornering performance with intermittent fault at mu = 1

Fig. 11. Cornering performance with intermittent fault at mu = 0.62 without ESC

In Fig. 12 the uncontrolled scenario at reduced mu is attempted to be controlled with an ESC control algorithm. The resulst demonstrate that the vehicle can be controlled and provide safe performance as the added yaw rate (2.76º to -2.76º) and added body slip angle (0.57º to -0.19º) control peak limits are close to Neukum's recommendations. The oscilations of the yaw rate are caused by the delayed response of the driver attempting to control the yaw rate of the vehicle. Because of this delay in the driver's feedback, the yaw rate becomes excited by the driver's input corresponding to undamped oscilation with constant amplitude. The small gain steering angle control applied by the driver corresponds to the emotional response of the driver to maintain the initial steering wheel relative to the chosen path. This is despite the steering wheel feedback torque as it has been concluded from experimental results.
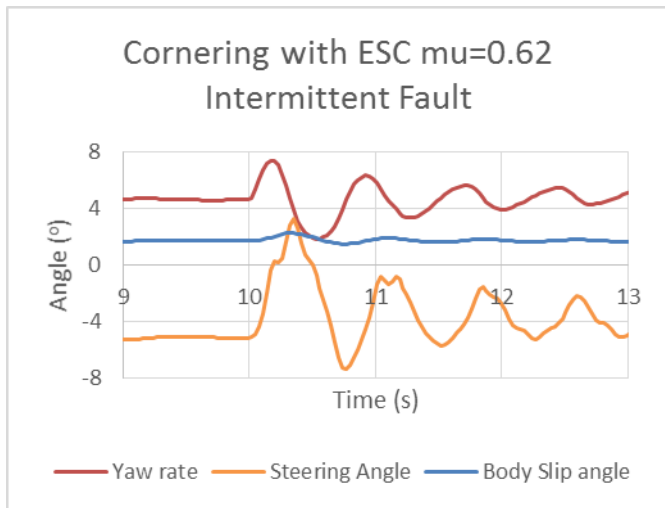
Fig. 12. Cornering performance with intermittent fault at mu = 0.62 with ESC

Fig. 13 demonstrates an attempt to tune the driver model heading feedback by reducing the filter frequency to 0.5Hz and significantly increasing the damping ratio causing the driver to respond slower to heading deviations. Despite the slower response of the yaw rate osclation frequency has increased even if the steering angle curve is now smoother.
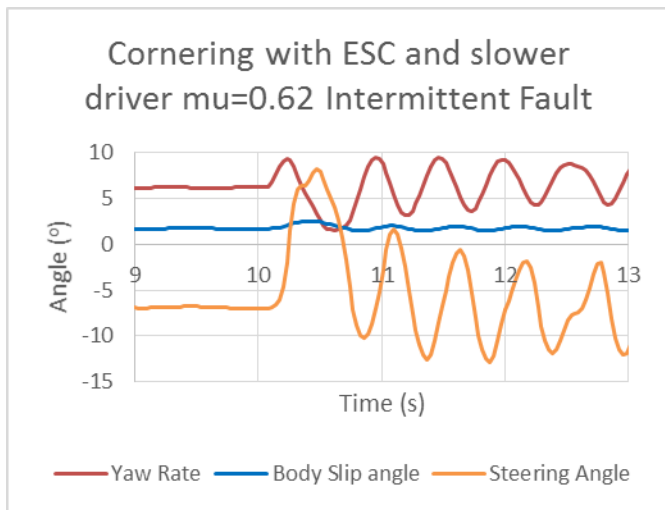

Fig. 13. Cornering performance with intermittent fault at mu = 0.62 without ESC

At this stage it is important to understand that the cornering scenario at mu = 0.62 is performed while the tyres are already close to their friction limit and within their highly non-linear cornering stiffness. A scenario like this would be difficult to control even with skilled physical driver on a vehicle with such behaviour on the friction limit. Fig. 14 demonstrates an a cornering scenario at mu = 0.7, with and without ESC where with the same driver model the ESC manages succesfully to control the yaw rate of the vehicle.
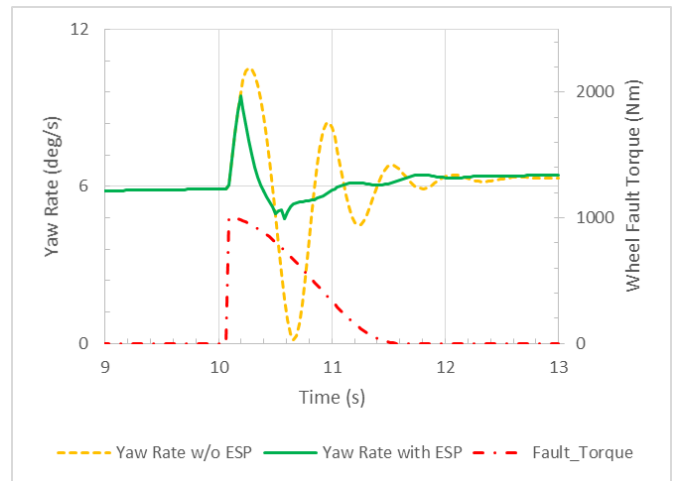

Fig. 14. Cornering performance with intermittent fault at mu = 0.65 with and without ESC

4.2.2 Disabled Motors fault

Performing the same coefficient of friction as at the intermittent fault scenarios, the disabled motors fault is deomnstrated below. Fig. 15 results at mu = 1 of the yaw rate and body slip angle indicate that there is no controllability issue. The range of the added yaw rate is 2.42º to -0.87º and added body slip angle is 0.48º to -0.03º which are within Neukum's recommendations. The disturbance is also smaller compared to the intermittent scenario. This is because the driver is already controlling the vehicle with recuded lateral forces at the rear axle, as the fault changes the direction of the applied torque, due to the motor similar limitation of torque on both driving and disabled when it is operating at the specific angular velocity corresponding to 150km/h. The longitudinal load transfer however is affecting the balance of the front to rear vertical forces causing a further reduction of the friction limit on the rear tyres.
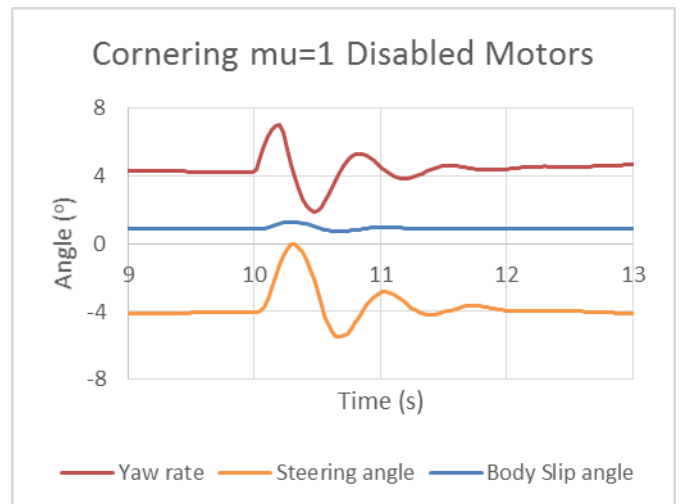

Fig. 15. Cornering performance with disabled motors at mu = 1

The above is also demonstrated at reduced mu of 0.62 in Fig. 16 where the vehicle does not need the use of ESC to maintain stability. In this scenario, the added yaw rate range is 3.87º to -3.83º and added body slip angle of 0.90º to -0.32º which is beyond Neukum's recommendations, however, the vehicle manages to return back to its initial state within reasonable time after the start of the fault.
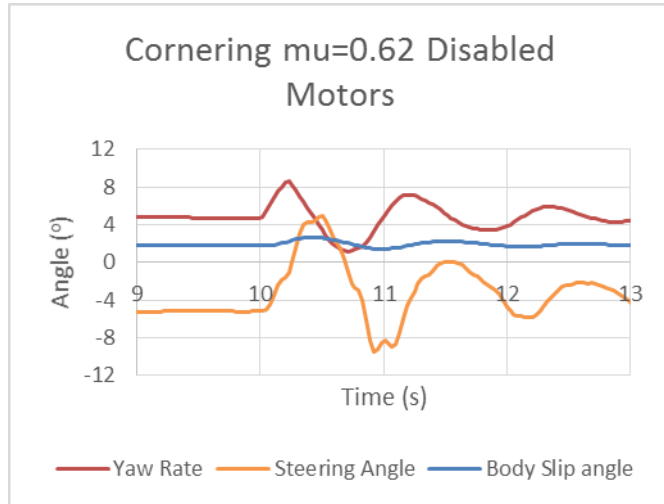

Fig. 16. Cornering performance with disabled motors at mu = 0.62 without ESC

5. CONCLUSIONS

Two different fault scenarios have been demonstrated in both high and low mu surface. The intermittent fault proved to cause significant consern of controlability especially at low mu where even skilled drivers will have difficulty controlling the vehicle without an ESC. A driver model sensitivity study is performed at the low mu cornering event with ESC in attempt to demonstrate the relationship between driver behaviour and ESC operation. From further simulations it is understood that the better the driver manages to hold the steering angle during the fault the better the ESC will manage to control the vehicle. Once the driver starts to attempt to control the heading of the vehicle by his feedback, the system enters a loop of non decaying yaw rate oscilation that can become unstable in real life.

The significant difference of the applied faults during cornering causing the intermittent fault to be less controllable during low mu scenarios is caused by the suddent change of the balance of the lateral forces applied by the tyres. This suddent change causes greater yaw momentum and grater yaw rate overshoot that can be very difficult to control at low mu due to high slip angle of the tyre close or even beyond the friction limit. On the other hand, the disabled motors scenario by inverting the applied torque direction causes less overshoot due to the small yaw momentum applied and the similar lateral forces applied by the tyres, where the slip angle of the tyres do not exceed the friction limit.

Most of the investigated scenarios can be considered to be within or just above the "disturbing" operational limits of yaw rate according to Neukum but should be considered safe.

REFERENCES

Alirezaei, M., Kanarachos, S., Scheepers, B., Maurice, J.P. (2013). Experimental evaluation of optimal Vehicle Dynamic Control based on the State Dependent Riccati Equation technique, *Proceedings of the American Control Conference*, art. no. 6579871, pp. 408-412

Ellims, M., Monkhouse, H., Harty, D., and Gade, T. (2013). "Using Vehicle Simulation to Investigate Controllability," *SAE Int. J. Alt. Power.* 2(1), pp.18-36.

Harty, D., Gade, T. (2013). *"Review of Stability Risks with In-Wheel Motors".*

Hirano, Y. (2012). Integrated vehicle control of an in-wheel-motor vehicle to optimize vehicle dynamics and energy consumption, *Proceedings of the World Congress on Intelligent Control and Automation (WCICA)*, art. no. 6358264, pp. 2335-2339.

ISO 26262: 2011 (2011), Road vehicles -Functional safety.

Kanarachos, S.A. (2009). A new method for computing optimal obstacle avoidance steering manoeuvres of vehicles, *International Journal of Vehicle Autonomous Systems*, Vol. 7 (1-2), pp. 73-95.

Neukum, A., Ufer, E., Paulig, J., & Krüger, H.-P. (2008). Controllability of superposition steering system failure. In ATZ/TUEV SUED (Ed.), steering.tech. Available: http://www.psychologie.uni-wuerzburg.de/izvw/texte/2008_Neukum_etal_Controllability_of_superposition_steering_failures.pdf.

Reinelt, W., Lundquist, C. (2006). Controllability of active steering system hazards: From standards to driving tests, *SAE Technical Papers*.

Watts, A., Vallance, A., Whitehead, A., Hilton, C., Fraser, A. (2010). The technology and Economics of In-Wheel Motors, *SAE International Journal of Passenger Cars - Electronic and Electrical Systems*, Vol. 3 (2), pp. 37-54.

Weitzel, Alexander1; Winner, Hermann (2013). Controllability assessment for unintended reactions of active safety systems, *Proceedings of the 23rd International Technical Conference on the Enhanced Safety of Vehicles* (ESV), Available: http://www-esv.nhtsa.dot.gov/Proceedings/23/files/23ESV-000042.PDF